PHYSICAL REVIEW A VOLUME 46, NUMBER 9 1 NOVEMBER 1992

General theoretical approach to Coulombic three-body systems by the hyperspherical formalism

H. T. Coelho
Departamento de Física, Universidade Federal de Pernambuco, 50739 Recife, Pernambuco, Brazil

J. J. De Groote and J. E. Hornos
Instituto de Física e Química de São Carlos, Universidade de São Paulo, 13560 São Carlos, São Paulo, Brazil

(Received 13 August 1991; revised manuscript received 19 November 1991)

Coulombic three-body systems are investigated using the hyperspherical adiabatic approach. By using a suitable variable $z=\tan(\alpha/2)$ in the angular differential equation for the determination of the potential curves, we are able to obtain stable series-expansion solutions, valid for small and large values of the hyperspherical radius. The analysis of the mathematical singularities of the differential equations in the variable z offers an insight into the physics of the problem and into the determination of stable converging solutions as well. In order to illustrate our investigation, we apply this study to several carefully chosen systems: He, $dd\mu$, d_2^+, and excitons bound to a Coulomb center in different semiconductors.

PACS number(s): 31.10.+z, 03.65.Ge

I. INTRODUCTION

The study of three-body systems interacting via Coulomb forces is of great importance due to a large variety of physical systems found in atomic and molecular physics. In atomic physics the nuclear motion is neglected and the system is approximately described by the independent-electron model, where each electron is subject to an averaged screening potential. In the case of molecular physics, the traditional Born-Oppenheimer (BO) approximation is mostly used. Due to the large difference between the masses of protons and electrons, the BO approximation is well suited. In this approximation each internuclear separation is taken as fixed for the motion of the electron. These two approximate methods have their own limitations [1]. In the nonrelativistic case the hyperspherical approach [2] (HA) appears to be a method to treat three-body systems in a rigorous and transparent way. Normally the HA leads to a difficult solution of a coupled system of differential equations of infinite dimension. This problem becomes even more severe if Coulomb forces are present [3]. A well-established procedure [4–10] to handle such physical systems within the HA is the hyperspherical adiabatic approach (HAA). This is similar to the BO approximation in diatomic molecules. The Schrödinger equation in hyperspherical coordinates is solved at each fixed hyperradius R to generate a family of effective potential curves. These potential curves, similar to the molecular potentials, contain essential information about the structure of the three-body system. As a result, we are required to search for a procedure to obtain in an efficient way the potentials $U_\lambda(R)$ for the whole range of R and for a variety of physical systems. The literature [4–10] is full of works illustrating the use of the HAA from the atomic to the nuclear scale. Technical problems involve the process of obtaining $U_\lambda(R)$, mostly because of the slow convergence of the hyperspherical harmonic functions. For short-range forces, $U_\lambda(R)$ is successfully obtained by diagonalization procedures [8]. However for long-range forces this procedure appears not to be practical, mostly because of the highly oscillating Jacobi polynomials present in the hyperspherical-harmonic functions, generating slow convergence. This slow convergence is also attributed to the fact that the asymptotic solutions are not easily expanded in terms of hyperspherical harmonics. A way to solve this difficulty is presented in this paper. Instead of the diagonalization procedure, we look directly for solutions of the angular differential equations. This is partially accomplished by incorporating the properties of the differential equations in the small- as well as large-R limits. These differential equations depend only on the hyperspherical angle α and contain trigonometric functions as coefficients of the derivatives. The hyperspherical radius R is also present but taken as the adiabatic variable. In this paper we present a general formulation of the Coulombic three-body problem in the spirit of the authors of Ref. [7]. In that reference only the simplest system, the He atom, was considered. By developing an analytical solution of the angular differential equations in a power-series expansion in a suitable variable, namely, $z=\tan(\alpha/2)$, we can transform the differential equations to a form where the Cauchy theorem can be applied. This basically implies that the above-mentioned coefficients become rational functions in the new variable z. Another resulting advantage of this transformation is to incorporate the topological properties of the mathematical singularities of the differential equations in order to obtain physical insights and generate stable converging solutions.

The next step after the precise determination of $U_\lambda(R)$ is to obtain the energies and wave functions of Coulombic three-body systems. That is achieved by solving a one-dimensional Schrödinger-type equation in the variable R. In the HAA one makes use of a recently proved set of basic inequalities [12], which provide for the first time a

lower-bound–upper-bound relation for the ground-state energies.

For the purpose of this work we use mass-weighted hyperspherical coordinates, to study Coulombic systems of arbitrary masses. Concerning the location of the singularities, we have carefully chosen several systems to illustrate our approach: He, $dd\mu$, $d_2{}^+$, and a three-particle complex corresponding to an exciton bound to a Coulomb center in a semiconductor. In the last case, results are calculated as a function of the mass ratio of the hole and electron, for several semiconductor materials.

In Sec. II we outline the HAA. In Sec. III we discuss how to obtain the potentials $U_\lambda(R)$. In Sec. IV we study several different Coulombic three-body systems, one of them (excitons) of varying mass. Finally, in Sec. V we present our conclusions. Some sections are divided into subsections in order to make the article more pedagogical. An appendix is included for completeness of the sections.

II. HYPERSPHERICAL ADIABATIC APPROACH

A. Hyperspherical formalism

Jacobi coordinates form an appropriate set for the three-body problem. Let $\mathbf{r}_i$ be the coordinate of particle i in the laboratory frame, which has mass m_i. Let $\boldsymbol{\rho}_1$ be the vector from particle 1 to particle 2 with reduced mass $\mu_1=m_1m_2/(m_1+m_2)$. The second vector $\boldsymbol{\rho}_2$ is from the center of mass (c.m.) of particles 1 and 2 to particle 3, with reduced mass $\mu_2=(m_1+m_2)m_3/(m_1+m_2+m_3)$. This procedure can easily be generalized to N-body systems [11]. It is also useful to introduce a set of mass-weighted coordinates $\boldsymbol{\xi}_i=(\mu_i/\mu)^{1/2}\boldsymbol{\rho}_i$, where μ is an arbitrary mass. The choice of Jacobi coordinates is not unique [11], but normally dictated by the nature of the physical problem under consideration.

We can explicitly set down our choice of coordinates used in this work:

$$\begin{aligned}\boldsymbol{\xi}_0&=(m_1\mathbf{r}_1+m_2\mathbf{r}_2+m_3\mathbf{r}_3)/(m_1+m_2+m_3)\ ,\\ \boldsymbol{\xi}_1&=(\mu_1/\mu)^{1/2}(\mathbf{r}_1-\mathbf{r}_2)\ ,\\ \boldsymbol{\xi}_2&=(\mu_2/\mu)^{1/2}\left[\frac{m_1\mathbf{r}_1+m_2\mathbf{r}_2}{m_1+m_2}-\mathbf{r}_3\right]\ .\end{aligned}\tag{1}$$

The Hamiltonian of our three-body system interacting via Coulomb forces is written as

$$H=-\frac{\hbar^2}{2(m_1+m_2+m_3)}\nabla^2_{\xi_0}-\frac{\hbar^2}{2\mu}(\nabla^2_{\xi_i}+\nabla^2_{\xi_2})+V(\xi_1,\xi_2)\ ,\tag{2}$$

where

$$V(\xi_1,\xi_2)=\left[\frac{\mu_1}{\mu}\right]^{1/2}\frac{q_1q_2}{\xi_1}+\frac{m_1}{\sqrt{\mu\mu_1}}\frac{q_1q_3}{|\xi_1+\eta_+\xi_2|}+\frac{m_2}{\sqrt{\mu\mu_1}}\frac{q_2q_3}{|\xi_1-\eta_-\xi_2|}\tag{3}$$

and

$$\begin{aligned}\eta_+&=[m_1(m_1+m_2+m_3)/m_2m_3]^{1/2}\ ,\\ \eta_-&=[m_2(m_1+m_2+m_3)/m_1m_3]^{1/2}\ .\end{aligned}\tag{4}$$

The symbols q_i stand for the particle electric charges. Notice that the use of Jacobi coordinates separated the c.m. motion in the kinetic-energy operator. In this way we can consider only the resulting Schrödinger equation in the c.m. At this point it is appropriate to introduce hyperspherical coordinates by defining a hyperspherical radius R,

$$R^2=\xi_1^2+\xi_2^2\ ,$$

and a hyperspherical angle α,

$$\begin{aligned}\xi_1&=R\sin\alpha\ ,\\ \xi_2&=R\cos\alpha\ ,\quad 0\le\alpha\le\pi/2\ .\end{aligned}\tag{5}$$

The Schrödinger equation $H\Psi=E\Psi$ in hyperspherical coordinates can be written as [7]

$$\left[\frac{\partial^2}{\partial R^2}-\frac{U(R,\Omega)-\frac{1}{4}}{R^2}+\varepsilon\right]\psi(R,\Omega)=0\ ,\tag{6}$$

where $\varepsilon=(2\mu/\hbar^2)E$, E being the energy eigenvalue, and $\Omega=\{\alpha,\hat{\xi}_1=(\theta_1,\varphi_1),\hat{\xi}_2=(\theta_2,\varphi_2)\}$. Notice that $\psi(R,\Omega)$ is the renormalized wave function given by $\psi(R,\Omega)=R^{5/2}\sin\alpha\cos\alpha\Psi(R,\Omega)$. To define $U(R,\Omega)$, let us call

$$U(0)=-\frac{\partial^2}{\partial\alpha^2}+\frac{\hat{l}_1^2(\hat{\xi}_1)}{\sin^2\alpha}+\frac{\hat{l}_2^2(\hat{\xi}_2)}{\cos^2\alpha}\ .\tag{7}$$

The quantities $\hat{l}_i^2(\hat{\xi}_i)$ $(i=1,2)$ stand for the usual angular-momentum operators. Defining $v=(2\mu/\hbar^2)V$ and $V(R,\Omega)=\hat{V}(\alpha,\theta)/R$, where

$$\begin{aligned}\hat{V}(\alpha,\theta)=&\left[\frac{\mu_1}{\mu}\right]^{1/2}\frac{q_1q_2}{\sin\alpha}\\ &+\frac{m_1}{\sqrt{\mu\mu_1}}q_1q_3/(\sin^2\alpha+\eta_+^2\cos^2\alpha\\ &\qquad+\eta_+\sin2\alpha\cos\theta)^{1/2}\\ &+\frac{m_2}{\sqrt{\mu\mu_1}}q_2q_3/(\sin^2\alpha+\eta_-^2\cos^2\alpha\\ &\qquad-\eta_-\sin2\alpha\cos\theta)^{1/2}\ ,\end{aligned}\tag{8}$$

and $\cos\theta=\hat{\xi}_1\cdot\hat{\xi}_2$, we finally have a useful relation:

$$U(R,\Omega)=U(0)+R^2v(R,\Omega)=U(0)+R\hat{v}(\alpha,\theta)\ .\tag{9}$$

B. Hyperspherical adiabatic approach

To solve Eq. (6) we can use a procedure known as the hyperspherical adiabatic approach with R treated as an adiabatic parameter. A revision of the HAA can be found in Refs. [4–11]. The idea is to expand ψ as follows:

$$\psi(R,\Omega)=\sum_\lambda F_\lambda(R)\Phi_\lambda(R,\Omega)\ ,\tag{10}$$

where the channel function Φ_λ satisfies the eigenvalue equation

$$U(R,\Omega)\Phi_\lambda(R,\Omega)=U_\lambda(R)\Phi_\lambda(R,\Omega) \tag{11}$$

for fixed R. The set of quantum numbers required to label the channel functions, here represented by λ, will be discussed in the next section. $F_\lambda(R)$ satisfies the equation

$$\left[\frac{d^2}{dR^2}-\frac{U_\lambda(R)-\frac{1}{4}}{R^2}+\varepsilon_\lambda\right]F_\lambda(R)+\sum_{\lambda'}W_{\lambda\lambda'}(R)F_{\lambda'}(R)=0\ , \tag{12}$$

where the nonadiabatic terms are given by

$$W_{\lambda\lambda'}=2P_{\lambda\lambda'}(R)\frac{d}{dR}+Q_{\lambda\lambda'}(R)\ , \tag{13}$$

where

$$\begin{aligned}P_{\lambda\lambda'}(R)&=\left\langle\Phi_\lambda\left|\frac{d}{dR}\right|\Phi_{\lambda'}\right\rangle\ ,\\ Q_{\lambda\lambda'}(R)&=\left\langle\Phi_\lambda\left|\frac{d^2}{dR^2}\right|\Phi_{\lambda'}\right\rangle\ .\end{aligned} \tag{14}$$

Differentiating $P_{\lambda\lambda'}(R)$ with respect to R, we can relate $P_{\lambda\lambda'}$ and $Q_{\lambda\lambda'}$ by

$$\frac{dP_{\lambda\lambda'}}{dR}=Q_{\lambda\lambda'}+R_{\lambda\lambda'}\ , \tag{15}$$

where

$$R_{\lambda\lambda'}(R)=\left\langle\frac{d\Phi_\lambda}{dR}\left|\frac{d\Phi_{\lambda'}}{dR}\right.\right\rangle\ . \tag{16}$$

If completeness is assumed $R_{\lambda\lambda'}=P^2_{\lambda\lambda'}$, and this furnishes a test for the completeness of the channel functions. The solution of Eq. (10) will furnish the eigenenergies and the wave functions of our system.

C. Adiabatic approximations and the basic inequalities

The set of coupled equations (12) is still exact. If truncation is done, the result is the so-called coupled adiabatic approximation (CAA) [6]. Neglecting the coupling terms $W_{\lambda\lambda'}(R)$, $\lambda\neq\lambda'$ in Eq. (12), the result is the uncoupled adiabatic approximation (UAA) [6]. In the UAA, the neglect of $W_{\lambda\lambda}(R)$ leads to the extreme adiabatic approximation (EAA) [6]. It can be proved [12] that the basic inequalities $\varepsilon_{\rm EAA}\le\varepsilon\le\varepsilon_{\rm CAA}\le\varepsilon_{\rm UAA}$ hold for the ground-state energies. The EAA is a lower bound while UAA and CAA are upper bounds. An inequality similar to that exists for the extreme Born-Oppenheimer approximation (BOA) [12], namely, $\varepsilon_{\rm BOA}\le\varepsilon$.

III. POTENTIAL CURVES

A. Basis functions

In order to solve Eq. (12) we first need to obtain the eigenpotentials $U_\lambda(R)$ from Eq. (11). We are interested in an efficient procedure to handle the numerical calculation such that the $U_\lambda(R)$'s are precisely obtained for the whole range of R and a wide range of masses of the three-body systems. In order to achieve it in an efficient way let us first look at the kinetic term of Eq. (7). That term has poles at $\alpha=0,\pi/2$ which are independent of the masses of the system. On the other hand, the Coulomb interaction term, given by Eq. (8), has poles at $\alpha=0$ and at $(\theta,\alpha)=(\pi,\alpha_+)$ and $(0,\alpha_-)$, where $\tan\alpha_\pm=\eta_\pm$. Thus the potential curves are obtained by considering regular solutions in the three regions $0\le\alpha\le\alpha_-$, $\alpha_-\le\alpha\le\alpha_+$, and $\alpha_+\le\alpha\le\pi/2$, and imposing continuity conditions at those boundary points.

In this kind of investigation it is important to select the appropriate angles and the corresponding harmonic functions as a basis for the problem. There exist different ways for selecting those angles. This was well studied by Smirnov and Shitikova [13]. Each possibility is identified with a possible chain in which the group O(6) can have its representation decomposed. We have chosen the chain

$$\begin{array}{ccccccc}\mathrm{O}(6) & \supset\mathrm{O}(3)\times\mathrm{O}(3) & \supset\mathrm{O}(3) & \supset\mathrm{O}(2)\\ \downarrow & \downarrow & \downarrow & \downarrow & \downarrow\\ \{nl_1l_2\} & \{l_1\} & \{l_2\} & \{L\} & \{M\}\end{array}\ , \tag{17}$$

which corresponds to the use of the tridimensional two-particle spherical harmonics. The channel functions are then written as

$$\Phi_\lambda(R,\Omega)=\sum_{l_1,l_2}(\sin\alpha)^{l_1+1}(\cos\alpha)^{l_2+1}\times\mathcal{Y}^{LM}_{l_1,l_2}(\hat{\xi}_1,\hat{\xi}_2)\mathcal{G}^\lambda_{l_1l_2}(R,\alpha)\ , \tag{18}$$

where $\mathcal{Y}^{LM}_{l_1l_2}$ is the usual two-particle coupled-orbital angular-momentum function ($|l_1-l_2|\le L\le l_1+l_2$ and $M=m_1+m_2$). The basis functions $\mathcal{G}^\lambda_{l_1l_2}(R,\alpha)$ at each R are obtained from the solution of Eq. (11).

The motivation for the choice given by Eq. (18) instead of other possibilities (such as Euler angles [11] or the canonical form used in nuclear physics [8]) is the following. The decomposition into two O(3) groups preserves the individuality of the effective particles with respect to the angular motion in the $(\theta_1,\varphi_1),(\theta_2,\varphi_2)$ manifolds. However the introduction of the variables α and R will account for the collective effects.

We note that the function $\mathcal{G}^\lambda_{l_1l_2}(R,\alpha)$ in Eq. (18) was not further expanded in any basis and will be calculated by a new method presented in this paper. In this point our approach differs from the usual techniques which are based on some kind of expansion using orthonormal polynomials [4–6,8–11] or another [11] set of functions with faster convergence properties.

The use of any kind of polynomial set assumes the separability of the variables α and R, i.e.,

$$\Phi_\lambda(R,\Omega)=\sum_{n,l_1,l_2}\chi^\lambda_{nl_1l_2}(R)\mathcal{Y}^{LM}_{nl_1l_2}(\Omega)\ , \tag{19}$$

where the complete orthonormal set $\{\mathcal{Y}^{LM}_{nl_1l_2}\}$ are hyperspherical harmonics [2]. The hyperspherical-harmonic approach corresponds to the prescription

$$\mathcal{G}^{\lambda}_{l_1 l_2}(R,\alpha)=\sum_n \chi^{\lambda}_{n l_1 l_2}(R) P_n^{l_1+1/2,l_2+1/2}(\cos(2\alpha)) , \quad (20)$$

where $P_n^{l_1+1/2,l_2+1/2}$ is the usual Jacobi polynomial. Thus the solution of Eq. (11) using (20) reduces the problem to a matrix diagonalization [6,8]. This way, although quite straightforward, has its limitations. For instance, a known limitation is due to the slow convergence because asymptotic solutions are not easily expanded in terms of $\mathcal{Y}^{LM}_{n l_1 l_2}(\Omega)$. This problem becomes very severe for long-range forces. However for short-range forces, such as the ones encountered in nuclear physics, this procedure is quite successful [8]. To overcome this problem in Coulombic three-body systems, Lin and Liu [11] considered a new basis function set but it has the disadvantage of not being an orthonormal set. In addition numerical difficulties are not completely removed for large-R values. The situation is in some sense dramatic if we notice that for a truncated calculation, using Jacobi polynomials, potential curves necessarily appear with wrong behavior for large R. In order to avoid these problems we shall solve directly the infinite set of differential equations obtained by substituting Eq. (18) into Eq. (11), namely,

$$\left\{\frac{d^2}{d\alpha^2}+2[(l_1+1)\cot\alpha-(l_2+1)\tan\alpha]\frac{d}{d\alpha}-U_\lambda(R)-(l_1+l_2+2)^2\right\}\mathcal{G}^{\lambda}_{l_1 l_2}(R,\alpha)-R\sum_{l_1' l_2'}\tilde{v}^{LM}_{l_1 l_2 l_1' l_2'}(\alpha)\mathcal{G}^{\lambda}_{l_1' l_2'}(R,\alpha)=0 , \quad (21)$$

where

$$\tilde{v}^{LM}_{l_1 l_2 l_1' l_2'}(\alpha)=(\sin\alpha)^{l_1'-l_1}(\cos\alpha)^{l_2'-l_2}\times\langle \mathcal{Y}^{LM}_{l_1 l_2}|\hat{v}|\mathcal{Y}^{LM}_{l_1' l_2'}\rangle . \quad (22)$$

An explicit expression for $\langle\hat{v}\rangle$ is given in the Appendix. To solve Eq. (21) we should be aware of the symmetries imposed in the hyperspherical-harmonic functions $\mathcal{G}^{\lambda}_{l_1 l_2}(R,\alpha)$. A discussion of this point can be seen for instance in Refs. [7] and [11].

B. Small- and large-R behaviors

It is remarkable that Eq. (21) admits exact solutions in the limit $R=0$. For instance, in that limit and using a new variable $\alpha=\alpha'/2$ and the transformation

$$\tilde{\mathcal{G}}^{\lambda}_{l_1 l_2}(R,\alpha)=(\sin\alpha)^{l_1+1}(\cos\alpha)^{l_2+1}\mathcal{G}^{\lambda}_{l_1 l_2}(R,\alpha) ,$$

we obtain

$$\left[-\frac{d^2}{d\alpha'^2}+\frac{4l_1(l_1+1)}{16\sin^2(\alpha'/2)}+\frac{4l_2(l_2+1)}{16\cos^2(\alpha'/2)}+\tfrac{1}{4}U_\lambda(0)\right]\mathcal{G}^{\lambda}_{l_1 l_2}(0,\alpha)=0 , \quad (23)$$

which compared with the canonical form of the Jacobi equation [14]

$$\left[-\frac{d^2}{d\alpha'^2}-\frac{1-4a^2}{16\sin^2(\alpha'/2)}-\frac{1-4b^2}{16\cos^2(\alpha'/2)}-\left[\lambda+\frac{a+b+1}{2}\right]^2\right]\mathcal{Q}^{(a,b)}_{\lambda}(\cos\alpha')=0 \quad (24)$$

has the regular solution

$$\mathcal{Q}^{(a,b)}_{\lambda}(\cos\alpha')=[\sin(\alpha'/2)]^{a+1/2}[\cos(\alpha'/2)]^{b+1/2}\times P^{(a,b)}_{\lambda}(\cos\alpha') , \quad (25)$$

where $P^{(a,b)}_{\lambda}$ are Jacobi polynomials.

Therefore the potential curves at $R=0$ have the form

$$U_\lambda(0)=(2n+j_1+j_2+2)^2 , \quad (26)$$

and the $\tilde{\mathcal{G}}$ functions are given by

$$\tilde{\mathcal{G}}^{LM}_{n j_1 j_2}(0,\alpha)=(\sin\alpha)^{l_1+1}(\cos\alpha)^{l_2+1}\times P_n^{l_1+1/2,l_2+1/2}(\cos(2\alpha))\delta_{l_1 j_1}\delta_{l_2 j_2} . \quad (27)$$

Since there are no spin interactions, the spatial wave function has well-defined quantum numbers, L, M, spin S, and parity. At $R=0$, we see explicitly from Eqs. (26) and (27) that the potential curves are labeled by $\lambda=(n,j_1,j_2)$. For notational simplicity we have omitted the conserved quantum numbers, L, M, S, and parity. The allowed values of j_1 and j_2 are dictated by the triangular relation with L and the required symmetry of the problem imposed by the parity. There is no restriction on the integer values of n. If the nonadiabatic couplings $W_{\lambda\lambda'}(R)$ [see Eq. (12)] are neglected, $\lambda=(n,j_1,j_2)$ will be conserved.

The inclination of the curve $U_\lambda(R)$ at $R=0$ is obtained by calculating the derivative of Eq. (11) and using Eq. (9). As a result, we get

$$\hat{v}(\alpha,\theta)\Phi_\lambda(0,\Omega)+[U(0)-U_\lambda(0)](\Phi_\lambda')_{R=0}=(U_\lambda')_{R=0}\Phi_\lambda(0,\Omega) . \quad (28)$$

The prime symbol on Φ_λ and U_λ indicates the derivative with respect to R of those quantities. Multiplying Eq. (28) by $\Phi^*_{\lambda'}(0,\Omega)$ and integrating over $d\Omega$ we obtain

$$\langle\Phi_{\lambda'}(R,\Omega)|\hat{v}(\alpha,\theta)|\Phi_\lambda(R,\Omega)\rangle_{R=0}+\langle\Phi_{\lambda'}(R,\Omega)|[U(0)-U_\lambda(R)]|\Phi_\lambda'(R,\Omega)\rangle_{R=0}=(U_\lambda')_{R=0}\delta_{\lambda'\lambda} . \quad (29)$$

For $\lambda'=\lambda$,

$$(U_\lambda')_{R=0}=\langle\Phi_\lambda|\hat{v}(\alpha,\theta)|\Phi_\lambda\rangle_{R=0} , \quad (30)$$

where $\lambda=(n,j_1,j_2)$.

For $\lambda'\neq\lambda$, using Eq. (14), we have

$$\langle \Phi_{\lambda'}|\hat{v}(\alpha,\theta)|\Phi_\lambda\rangle_{R=0} = -(U_{\lambda'}-U_\lambda)_{R=0}P_{\lambda'\lambda}(0) \quad (31)$$

or equivalently,

$$P_{\lambda'\lambda}(0) = -\langle \Phi_{\lambda'}|\hat{v}(\alpha,\theta)|\Phi_\lambda\rangle_{R=0}/(U_{\lambda'}-U_\lambda)_{R=0} . \quad (32)$$

The analysis for large R is discussed in Refs. [4,7,11].

C. Set of differential equations with rational coefficients

Although solutions for Eq. (21) in the variable α (for fixed R) exist, the form of that equation is not appropriate for the use of the Cauchy theorem. The reason lies in the nonpolynomial structure of the trigonometric functions which appear there and the intractability of the series expansions of such functions. Thus we have searched for a new variable which can transform Eq. (21) into a form whose coefficients are rational functions. Therefore analytical solutions can be obtained in the usual power-series expansion. That variable is $z=\tan(\alpha/2)$. As a result, the expansion coefficients given by recursion formulas can be calculated numerically for fixed values of R. In the variable z, Eq. (21) reads

$$\left[\frac{d^2}{dz^2}+\mathcal{P}_{l_1l_2}(z)\frac{d}{dz}+\mathcal{Q}_{l_1l_2}(R,z)\right]\mathcal{G}^\lambda_{l_1l_2}(R,z) + R\sum_{l_1',l_2'}\mathcal{R}_{l_1l_1'l_2l_2'}(z)\mathcal{G}^\lambda_{l_1'l_2'}(R,z)=0 , \quad (33)$$

where

$$\mathcal{P}_{l_1l_2}(z)=\frac{2}{1+z^2}\left[z+\frac{(l_1+1)(1-z^2)}{z}-\frac{4(l_2+1)z}{1-z^2}\right] , \quad (34)$$

$$\mathcal{Q}_{l_1l_2}(R,z)=-4[(l_1+l_2+2)^2+U_\lambda(R)]/(1+z^2)^2 - \left[\frac{\mu_1}{\mu}\right]^{1/2} q_1q_2\frac{2}{z(1+z^2)} , \quad (35)$$

and

$$\mathcal{R}_{l_1l_1'l_2l_2'}(z)=-\frac{4}{(1+z^2)^2}\left[\frac{2z}{1+z^2}\right]^{l_1'-l_1}\left[\frac{1-z^2}{1+z^2}\right]^{l_2'-l_2} \times\left[\frac{m_1}{\sqrt{\mu\mu_1}}q_1q_3\Delta^+_{l_1l_1'l_2l_2'}(z) + \frac{m_2}{\sqrt{\mu\mu_2}}q_2q_3\Delta^-_{l_1l_1'l_2l_2'}(z)\right] . \quad (36)$$

The expressions for Δ^+ and Δ^- are given in the Appendix. The singular points of Eq. (8) occur at $z_\pm=\tan(\alpha_\pm/2)$. The singular points of Eq. (33) are $z=0,\pm1,\pm i$. The singular points are drawn in the complex-z plane shown in Fig. 1. As $0\le\alpha\le\pi/2$, it is implied that $0\le z\le1$. Thus only the region $\mathrm{Re}(z)\ge0$ is of physical interest in the solution of Eq. (33). That equation can be solved by a local power-series method for the function $\mathcal{G}^\lambda_{l_1l_2}(R,z)$ in each interval $[0,z_-]$, $[z_-,z_+]$, and $[z_+,1]$. Its solution has an exponential behavior [7] for large R, which can be built in. The resulting series is therefore rapidly convergent. Another aspect of Eq. (33) is its behavior at small R. In order to get a polynomial form at $R=0$, we should introduce [7] a factor $(1+z^2)^s$, where $s=l_1+l_2+2-\sqrt{U_\lambda(0)}$, and $U_\lambda(0)$ is given by Eq. (26). That series-expansion procedure generates an algebraic set of recursion relations for the series coefficients. To obtain the recursion relations from Eq. (33) is straightforward but tedious, so a computer code was written to extract it algebraically without performing floating-point operations. The same code also generates a FORTRAN program to solve the relations on a μVAX computer. One of the advantages of this method is to isolate two types of error. One comes from the truncation of the solution of Eq. (33) through the series-convergence procedure for a maximum number N of terms, and the other appears in the successive inclusion of angular-momentum channels until a limit value $l_{\max}$. Thus the coefficients are numerically calculated in an exact way. That can be verified afterward using quadruple precision floating-point arithmetics. The procedure of calculation, once the truncation limits are stated, begins with a tentative value for the potential $U_\lambda(R)$ at a point R, selected in practice by the application of the Newton forward-difference method [14] to the previously calculated points. Once a good tentative point is selected, the recursion relations are solved for arbitrary initial conditions in the regions $[0,z_-]$ and $[z_+,1]$. The singular behavior of the differential equation in those points are then exactly incorporated in the algorithm without causing any error or instability. Finally the equations are solved in the intermediate region by imposing continuity conditions which will simultaneously select the regular combination of the already calculated independent solutions and the potential curve. The determinantal condition which emerges from the procedure described above is used for the update of the value of $U_\lambda(R)$ and the process continues until a desired precision (machine precision) is reached. The same strategy is then repeated for the next value of R. As a result we have controlled truncation errors. The fundamental property of the chosen variable z is that the differential equation can undergo an arbitrary translation transformation without losing its polynomial character. This fact allows us to select smaller grids in the z space different from the natural ones of the three regions. Hence the method described above can also be

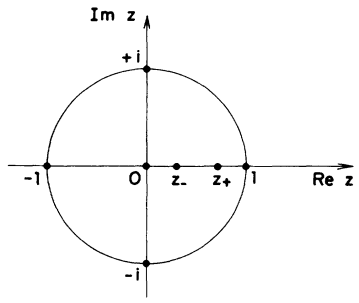

FIG. 1. Complex-z plane showing the singular points of Eq. (33).

combined with finite-difference techniques without losing its "exact" structure. This will be particularly important for systems with very different masses.

The singularities of Eq. (33) are shown in Fig. 1. The poles at ± 1 and $\pm i$ define a convergence circle of unity radius in which a regular solution at $z=0$ exists. Depending on the constituent masses of a given Coulombic system, the singularities z_+ and z_- will move along Re(z) defining two inner circles, in which Eq. (33) must be solved. Pole locations for several systems are shown in Table I. We can see that for systems with large mass ratio ($m_2/m_3 \gg 1$), like $d_2{}^+$, singularities will be pushed to the border limit, causing the known "large-mass" problem [9] in the calculation of the potential curves.

We should stress that machine precision in the truncation procedure was obtained with typical N values between 50 and 200 depending on the system, allowing us to carefully analyze the convergence trends in the angular-momentum expansion.

The solution of Eq. (33) will then give $U_\lambda(R)$ in a precise way. With this information at hand we can finally solve Eq. (12), by standard procedures, to obtain the energies and wave functions of the problem.

IV. APPLICATIONS

We give and discuss below the numerical results for several carefully chosen physical systems. This choice was mainly concerned with the topological locations of (z_-,z_+) when compared with the border singularities (0,1).

A. He

In order to appraise the accuracy of our approach, we present in Fig. 2 the potential curve for the helium ground state, calculated by our method and by matrix diagonalization. In the second method, the channel functions are expanded in 16, 20, 25, and 40 Jacobi polynomials, respectively. We can see that matrix diagonalization furnishes slow convergence even in the intermediate range of R. In addition, the asymptotic values of $U_0(R)/R^2$ are not correct, i.e., the truncated curves cross the ionization limit, resulting in unphysical results at large R.

In Table II we give the values of $U_0(R)$ at its minimum as a function of $l_{\max}=1,\ldots,30$, and $N=70,90,130$. The

TABLE I. Pole locations for several physical systems. Only (α_-,α_+) and (z_-,z_+) are listed.

System	α_-	α_+	z_-	z_+
He	$\pi/4$	$\pi/2$	0.414 21	1
$dd\mu$	1.406 77	α_-	0.848 09	z_-
$d_2{}^+$	1.559 13	α_-	0.988 40	z_+
InSb	1.317 51	$\pi/2$	0.774 11	1
ZnSe	1.182 85	$\pi/2$	0.671 62	1
CdS	1.150 26	$\pi/2$	0.648 23	1
ZnO	1.141 10	$\pi/2$	0.641 74	1
CdSe	1.132 22	$\pi/2$	0.635 49	1
$pd\mu$	1.437	1.308	0.874	0.767

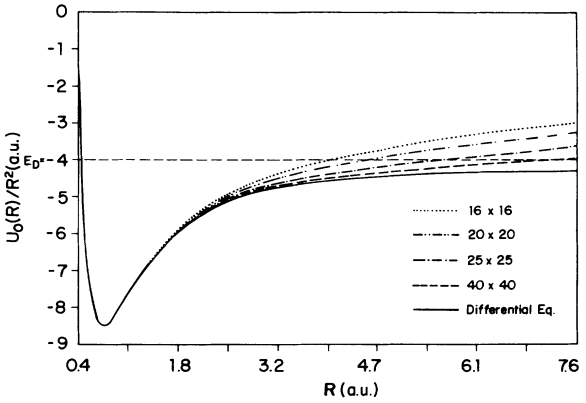

FIG. 2. Convergence trends of the solutions obtained by the diagonization procedure and by the solution of the angular differential equations for the He atom. The second method gives precise convergence. For each curve, obtained by the diagonization procedure, matrix dimensionality is given.

agreement between $N=90$ and 130 is of a few parts in 10^8. No difference can be observed in the potential curves if a larger value of N is taken. Numerical errors have been searched for using REAL* 16 precision and no difference was observed. The exponential factor mentioned in the preceding section causes a regular and stable behavior at large R even with a small number of terms in the series expansion. The angular-momentum convergence up to 30 channels is also shown in Table II. The convergence is much slower and we expect corrections of few parts in 10^8 if more angular-momentum channels are considered. The computation time is roughly proportional to $Nl_{\max}^2$.

B. Excitons

The behavior of excitons trapped by ions in semiconductors can be treated as the motion of dressed electrons and holes under the influence of the ion field in a medium of dielectric constant ε. Changing the semiconductor material, we can create different Coulombic systems with distinct mass ratios m_2/m_3. In Table III we list the properties of several semiconductors. In Fig. 3, we plot $U_0(R)/R^2$ for several semiconductor materials. The

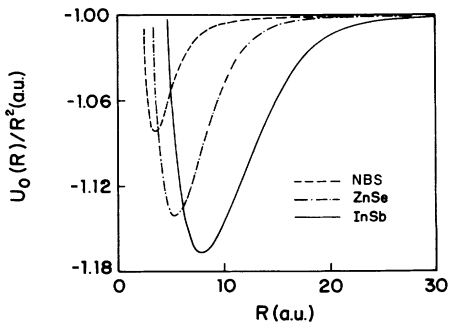

FIG. 3. Plot of $U_0(R)/R^2$ vs R for several semiconductor materials. The material "crit" is defined in the text. Units are in $\hbar=e^2/\varepsilon=m_e=1$.

TABLE II. Calculated values of $U_0(R)$ (in eV) at its minimum as a function of N (the maximum number of terms of the power-series expansion) and l_{max} [maximum value of the angular momentum $l_1=l_2$ $(L=0)$] for He.

l_{max} \ N	70	90	130
2	−8.482 315 532 110 19	−8.482 315 532 110 19	−8.482 315 532 110 192
3	−8.489 208 645 993 10	−8.489 208 645 993 10	−8.489 208 645 993 092
4	−8.490 957 921 633 46	−8.490 957 921 633 46	−8.490 957 921 633 461
5	−8.491 591 462 814 78	−8.491 591 462 814 78	−8.491 591 462 814 778
6	−8.491 873 637 481 07	−8.491 873 637 481 07	−8.491 873 637 481 055
7	−8.492 017 669 190 34	−8.492 017 669 190 17	−8.492 017 669 190 149
8	−8.492 098 663 479 05	−8.492 098 663 476 91	−8.492 098 663 476 909
9	−8.492 147 629 963 51	−8.492 147 629 945 65	−8.492 147 629 945 638
10	−8.492 178 945 377 02	−8.492 178 945 268 49	−8.492 178 945 268 362
11	−8.492 199 892 651 77	−8.492 199 892 203 62	−8.492 199 892 202 962
12	−8.492 214 428 870 31	−8.492 214 427 625 26	−8.492 214 427 621 516
13	−8.492 224 829 528 50	−8.492 224 827 097 76	−8.492 224 827 078 434
14	−8.492 232 465 960 52	−8.492 232 462 354 39	−8.492 232 462 276 760
15	−8.492 238 198 436 34	−8.492 238 193 733 97	−8.492 238 193 504 505
16	−8.492 242 586 660 84	−8.492 242 579 383 34	−8.492 242 578 877 736
17	−8.492 246 008 891 60	−8.492 245 992 084 67	−8.492 245 991 220 818
18	−8.492 248 733 649 87	−8.492 248 687 221 91	−8.492 248 686 020 558
19	−8.492 250 964 559 25	−8.492 250 843 761 33	−8.492 250 842 335 194
20	−8.492 252 865 365 12	−8.492 252 589 713 38	−9.492 252 588 186 838
21	−8.492 254 565 467 63	−8.492 254 018 432 37	−8.492 254 016 755 217
22	−8.492 256 148 091 78	−8.492 255 199 480 88	−8.492 255 196 956 057
23	−8.492 257 633 187 29	−8.492 256 186 304 52	−8.492 256 180 500 316
24	−8.492 258 976 017 81	−8.492 257 022 029 73	−8.492 257 006 698 077
25	−8.492 260 096 094 08	−8.492 257 743 904 41	−8.492 257 705 790 296
26	−8.492 260 927 508 91	−8.492 258 386 068 01	−8.492 258 301 298 996
27	−8.492 261 460 166 71	−8.492 258 979 708 37	−8.492 258 811 709 149
28	−9.492 261 745 286 47	−8.492 259 549 876 91	−8.492 259 251 683 967
29	−8.492 261 866 502 40	−8.492 260 109 798 49	−8.492 259 632 955 843
30	−8.492 261 902 349 78	−8.492 260 655 852 92	−8.492 259 964 987 300

word "crit" [17] appearing in Fig. 3 stands for a fictitious material for which there is no bound state. In the last two columns of Table III we show the calculated ionization energies in the EAA. We compare them with variational calculations done by other authors. The bound states of those systems are very close to the ionization threshold. They get closer to it as the mass ratio $m=m_h^*/m_e^*$ decreases. Notice that m_e^* and m_h^* are the dressed masses of the electron and the hole, respectively. The calculated energies, as we have proved elsewhere [12], should satisfy the basic inequalities. This is verified in Table III with the exception of InSb. In this case the considered number of angular-momentum channels was not large enough to achieve energy convergence. On the other hand a precise calculation concerning this problem was done for ZnSe where up to ten angular-momentum channels ($l=0,1,2,\ldots,9$) were considered in order to achieve convergence. The results for ZnSe are shown in Fig. 4. In Table IV the convergence is also studied for ZnSe for $N=80,100,120$ and l up to 9. As we expect, the convergence is in general slowed when the mass ratio departs from unity and the singularities approach the convergence limit. We can see that a relatively large number of channels should be considered in order to

TABLE III. Binding energies for several semiconductors. E_D is the dissociation energy. The superscripts refer to variational calculations. Notice that ε is the static dielectric constant of the material and the values are taken from Ref. [15].

Material	ε	m_e^*(amu)	m_h^*(amu)	m_e^*/m_h^*	E_D(meV)	$E-E_D$(meV)		$(E-E_D)/E_D$(%)	
InSb	16.80	0.02	0.30	0.067	0.9641	0.0893	0.0993[a]	9.26	10.30[a]
ZnSe	9.10	0.10	0.60	0.167	16.43	0.751	0.676[a]	4.57	4.12[a]
CdS	10.33	0.20	1.00	0.20	25.50	1.161	1.0[b]	3.60	3.10[b]
ZnO	8.50	0.24	1.14	0.21	45.19	2.357	1.9[b]	3.35	2.70[b]
CdSe	10.66	0.13	0.59	0.22	15.56	0.486	0.348[a]	3.12	2.23[a]

[a]See Ref. [15].
[b]See Ref. [16].

TABLE IV. The same as Table II for ZnSe, but energies are in meV.

l_{max} \ N	80	100	120
3	−18.286 645 253 633 47	−18.286 645 324 116 43	−18.286 645 324 932 39
4	−18.490 819 440 687 19	−18.490 819 927 211 56	−18.490 819 951 060 05
5	−18.611 726 842 749 93	−18.611 725 415 043 15	−18.611 725 662 805 09
6	−18.686 108 420 911 53	−18.686 084 527 574 57	−18.686 085 623 484 81
7	−18.733 710 953 017 42	−18.733 600 636 118 52	−18.733 602 574 767 91
8	−18.765 394 594 219 11	−18.765 079 124 516 75	−18.765 076 931 027 69
9	−18.787 314 724 301 17	−18.786 635 961 872 30	−18.786 613 260 292 23

reach convergence. With our results, the variational calculations [15,16], and the knowledge of the basic inequalities [12], we can establish lower- and upper-bound relations for those systems. However one should have in mind that the lower-bound character of the EAA will only be granted if convergence in the angular momentum is achieved.

C. $dd\mu$ and d_2^+

Muon catalyzed fusion [18–20] has in part motivated us in the calculation of the potential curves of the quasilinear $dd\mu$ molecule. Jacobi coordinates (ξ_1,ξ_2) are chosen such that one of them, namely, ξ_1, is taken as the nuclear separation (deuteron-deuteron distance). With the use of this "Born-Oppenheimer"-type approximation, the potential curve goes to zero as R gets large as it should. The convergence trend of the potential curve is shown in Fig. 5. The graphs are for 1–5 channels. In this case, due again to different masses, the convergence is achieved only with a precision of 10 eV. The consideration of $dd\mu$ and d_2^+ in this work is due to the fact that they are the ones most troublesome to analyze within the HAA. Therefore this is a crucial test for the use of the present techniques. The $dd\mu$ system can only be handled by the present approach if the finite-difference technique mentioned in the last section is used. In Table V we give the values of $U_0(R)/R^2$ at its minimum as a function of N and l_{max}.

As a final example we give the preliminary results for the d_2^+ molecule. The potential curve for $U_0(R)/R^2$ is shown in Fig. 6. We have chosen the system d_2^+ because it illustrates well the topology of the problem. Its singularity ($z_-=z_+$) is very close to $z=1$ (see Fig. 1), causing slow convergence in the series, requiring therefore more computer CPU time. The inclusion of more channels should improve the results, as it happened for the $dd\mu$ system. We are presently working on this calculation.

V. CONCLUSIONS

We present in this paper a general method of handling the troublesome Coulombic three-body systems through the hyperspherical adiabatic approach. For long-range forces no matter what method is chosen we might face convergence problems in the determination of the solutions. This may not be different even if the exact HAA is

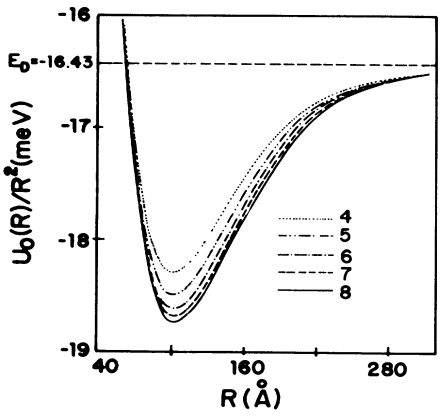

FIG. 4. Potential curves as a function of the number of angular channels for ZnSe. Graphs here are given for 4–8 channels. Note that convergence requires the use of a large number of channels in the calculation. The deeper the curve the larger the number of channels required.

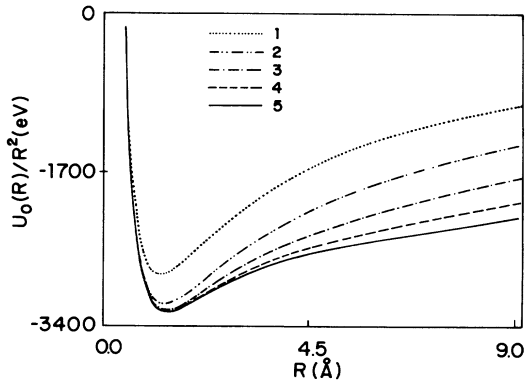

FIG. 5. Potential curves as a function of the number of angular channels for $dd\mu$. Graphs here are given for 1–5 channels. Note that convergence requires the use of a large number of channels in the calculation. The deeper the curve the larger the number of channels required. The abscissa is the hyperspherical radius multiplied by $(2m_e/m_D)^{1/2}$ in order to establish a correspondence with the internuclear separation [see Eq. (1)]. R is in units of $\hbar^2/m_\mu e^2$.

TABLE V. Calculated values of $U_0(R)/R^2$ at its minimum as a function of N (the maximum number of terms of the power-series expansion) and l_{max} [maximum value of the angular momentum $l_1=l_2(L=0)$] for $dd\mu$.

l_{max} \ N	150	250	350	450
1	2816.118 270 341	2816.118 270 612	2816.118 270 612	2816.118 270 612
2	3154.341 168 834	3154.340 757 821	3154.340 757 821	3154.340 757 821
3	3219.416 388 365	3219.397 817 965	3219.397 819 028	3219.397 819 024
4	3237.506 651 807	3237.413 893 992	3237.413 849 613	3237.413 846 365
5	3244.219 681 145	3244.050 239 226	3244.049 625 397	3244.049 383 539

used. However by using a suitable variable, namely, $z=\tan(\alpha/2)$, Eq. (11) can be transformed into the important Eq. (33), which can be solved by a power-series expansion, giving rise to a stable and converging solution valid for small and large values of the hyperspherical radius R. The solution of Eq. (33) furnishes simultaneously and in a precise way $U_\lambda(R)$, which is basically the ultimate physical goal in the calculation of the Coulombic three-body systems. Analysis of the mathematical singularities of Eq. (33) offers an insight into the physics of the problem and in the determination of stable converging solutions as well.

The approach presented here is exact, theoretically transparent, and general enough to be used successfully in the description of three-body systems. Although developed here for long-range forces, it can be applied to intermediate- and short-range forces as well. This version of the HAA permits the exact calculation of potential curves, binding energies, resonances, and possibly scattering states. In order to illustrate our approach we have considered several Coulombic three-body systems: He, $dd\mu$, $d_2{}^+$, and excitons bound to a Coulomb center in different semiconductors.

The theoretical description of Coulombic three-body systems is no longer hampered by lack of an efficient method for calculating potential curves and channel functions. The approach presented in this work, in our view, will prove to be useful.

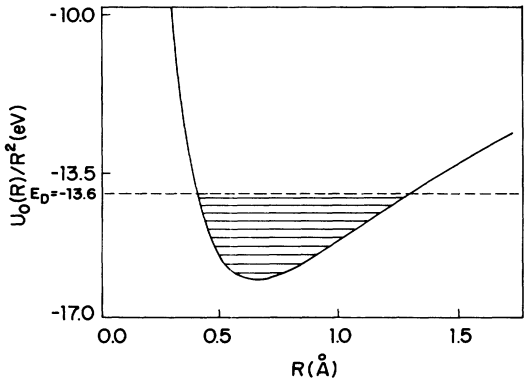

FIG. 6. Plot of $U_0(R)/R^2$ vs R for $d_2{}^+$. Horizontal lines represent some of the lowest bound states supported by $U_0(R)$. They are below the dissociation energy $E_D=-13.605$ eV. The abscissa is the hyperspherical radius multiplied by $(2m_e/m_D)^{1/2}$ in order to establish a correspondence with the internuclear separation [see Eq. (1)]. R is in units of $\hbar^2/m_\mu e^2$.

ACKNOWLEDGMENTS

This work was partially supported by Conselho Nacional de Desenvolvimento Científico e Tecnológico (CNPq), Financiadora de Estudos e Projetos (FINEP), Fundação de Amparo à Pesquisa de São Paulo (FAPESP), and Fundação de Amparo à Ciência e Tecnologia de Pernambuco (FACEPE) (Brazilian agencies).

APPENDIX: EVALUATION OF THE CHANNEL MIXING COEFFICIENTS

To calculate the matrix elements of v in Eq. (22), because of the form of Eq. (8), we first need to evaluate the tensor

$$\mathcal{T}^{LM\pm}_{l_1l_1'l_2l_2'}(\alpha)=\int d\hat{\xi}_1 d\hat{\xi}_2[\mathcal{Y}^{LM}_{l_1'l_2'}(\hat{\xi}_1,\hat{\xi}_2)]^* \times(\sin^2\alpha+\eta_\pm^2\cos^2\alpha \pm\eta_\pm\sin2\alpha\cos\theta)^{-1/2}\mathcal{Y}^{LM}_{l_1l_2}(\hat{\xi}_1,\hat{\xi}_2)\ . \tag{A1}$$

Notice that the square-root term can always be written in the form

$$f(1+t^2\pm2tx)^{-1/2}\ ,\quad x=\cos\theta\ , \tag{A2}$$

where the expressions for f and t are given in Table VI.

We also know by the definition of the Legendre polynomials [14] that

$$(1+t^2\pm2tx)^{-1/2}=\sum_{L'=0}^{\infty}(\mp)^{L'}t^{L'}P_{L'}(x)\ ,\quad |t|<1\ . \tag{A3}$$

Because of the selection rules used below, the condition $|t|<1$ is not mandatory. Using the addition theorem for $P_L(x)$ and the fact that

$$\mathcal{Y}^{LM}_{l_1l_2}(\hat{\xi}_1,\hat{\xi}_2)=\sum_{m_1,m_2}\langle LM|l_1m_1l_2m_2\rangle Y_{l_1m_1}(\hat{\xi}_1)Y_{l_2m_2}(\hat{\xi}_2)\ , \tag{A4}$$

we obtain, after some straightforward algebra, the expression

TABLE VI. Expressions for t and f appearing in Eq. (A2).

	(+) sign		(−) sign	
α interval	f	t	f	t
$0\le\alpha\le\alpha_-$	$(\eta_+\cos\alpha)^{-1}$	$\tan\alpha/\eta_+$	$(\eta_-\cos\alpha)^{-1}$	$\tan\alpha/\eta_-$
$\alpha_-\le\alpha\le\alpha_+$	$(\eta_+\cos\alpha)^{-1}$	$\tan\alpha/\eta_+$	$(\sin\alpha)^{-1}$	$\eta_-\cot\alpha$
$\alpha_+\le\alpha\le\pi/2$	$(\sin\alpha)^-$	$\eta_+\cot\alpha$	$(\sin\alpha)^{-1}$	$\eta_-\cot\alpha$

$$\langle\hat{v}\rangle=\left[\frac{\mu_1}{\mu}\right]^{1/2}\frac{q_1q_2}{\sin\alpha}\delta_{l_1l_1'l_2l_2'}+\frac{m_1}{\sqrt{\mu\mu_1}}q_1q_3\Delta^+_{l_1l_1'l_2l_2'}(\alpha)+\frac{m_2}{\sqrt{\mu\mu_2}}q_2q_3\Delta^-_{l_1l_1'l_2l_2'}(\alpha)\ , \tag{A5}$$

where

$$\Delta^{\pm}_{l_1l_1'l_2l_2'}(\alpha)=\sum_{L'}(\pm)^{L'}C^{LL'}_{l_1l_1'l_2l_2'}\mathcal{D}^{\pm}_{L'}(\alpha) \tag{A6}$$

and

$$C^{LL'}_{l_1l_1'l_2l_2'}=(-)^{L+L'}[(2l_1+1)(2l_1'+1)(2l_2+1)(2l_2'+1)]^{1/2}\begin{pmatrix}l_1 & l_1' & L'\\ 0 & 0 & 0\end{pmatrix}\begin{pmatrix}l_2 & l_2' & L'\\ 0 & 0 & 0\end{pmatrix}\begin{Bmatrix}l_1 & l_2 & L\\ l_2' & l_1' & L'\end{Bmatrix}, \tag{A7}$$

where the usual 3-j and 6-j symbols appear. The $\mathcal{D}^{\pm}_{L'}$ terms are given by

$$\mathcal{D}^{\pm}_{L'}(\alpha)=\begin{cases}(\tan\alpha/\eta_\pm)^{L'}(\eta_\pm\cos\alpha)^{-1}\ , & 0\le\alpha\le\alpha_-\\ (\tan\alpha/\eta_+)^{L'}(\eta_+\cos\alpha)^{-1},(\eta_-\cot\alpha)^{L'}/\sin\alpha\ , & \alpha_-\le\alpha\le\alpha_+\\ (\eta_\pm+\cot\alpha)^{L'}/\sin\alpha, & \alpha_+\le\alpha\le\pi/2\ ,\end{cases} \tag{A8}$$

where $\tan\alpha_\pm=\eta_\pm$. In terms of the variable z, $\mathcal{D}^{\pm}_{L'}(z)$ can easily be obtained by noticing that $\tan\alpha=2z/(1-z^2)$, $\cot\alpha=(1-z^2)/2z$, $(\sin\alpha)^{-1}=(1+z^2)/2z$, and $(\cos\alpha)^{-1}=(1+z^2)/(1-z^2)$.

[1] Z. Chen and C. D. Lin, Phys. Rev. A **42**, 18 (1990).

[2] Yu. A. Simonov, in *Proceedings of the International Symposium on the Present Status and Novel Developments in the Nuclear Many-body Problems, Rome, 1972,* edited by F. Calogero and C. Ciofi degli Atti (Editrice Compositori, Bologna, 1973), p. 527; L. M. Delves, Nucl. Phys. **9**, 391 (1959); Nucl. Phys. **20**, 268 (1962); W. Zickendrath, Ann. Phys. (N.Y.) **35**, 18 (1965); Phys. Rev. **159**, 1448 (1967); F. T. Smith, *ibid.* **120**, 1058 (1960).

[3] M. I. Haftel and V. B. Mandelzweig, Phys. Rev. A **38**, 5995 (1988).

[4] J. H. Macek, J. Phys. B **1**, 831 (1968).

[5] J. H. Macek, Phys. Rev. A **31**, 2162 (1985); J. Macek and K. A. Jerjian, *ibid.* **33**, 233 (1986).

[6] V. P. Brito, H. T. Coelho, and T. K. Das, Phys. Rev. A **40**, 3346 (1989); S. K. Adhikari, V. P. Brito, H. T. Coelho, and T. K. Das, Nuovo Cimento B (to be published).

[7] J. E. Hornos, S. W. MacDowell, and C. D. Caldwell, Phys. Rev. A **33**, 2212 (1986).

[8] H. T. Coelho, T. K. Das, and M. R. Robilotta, Phys. Rev. C **28**, 1812 (1983); T. K. Das, H. T. Coelho, and M. Fabre de la Ripelle, Phys. Rev. C **26**, 2281 (1982).

[9] C. H. Greene, Phys. Rev. A **23**, 661 (1981).

[10] U. Fano, Rep. Prog. Phys. **46**, 97 (1983).

[11] C. D. Lin and X. Liu, Phys. Rev. A **37**, 2749 (1988).

[12] H. T. Coelho and J. E. Hornos, Phys. Rev. A **43**, 6379 (1991).

[13] Yu. F. Smirnov and K. V. Shitikova, Sov. J. Part. Nucl. **8**(4), 344 (1977) [Fiz. Elem. Chastits At. Yadra **8**, 847 (1977)].

[14] *Handbook of Mathematical Functions,* edited by M. Abramowitz and I. A. Stegun, 3rd ed. (Dover, New York, 1965), Chap. 22.

[15] M. Suffczynski, W. Gorzkowski, and X. Kowalczyk, Phys. Lett. **24A**, 453 (1967).

[16] T. Skettrup, M. Suffczynski, and W. Orzkowski, Phys. Rev. B **4**, 512 (1971).

[17] J. J. de Groote, J. E. Hornos, H. T. Coelho, and C. D. Caldwell, Phys. Rev. B **46**, 2102 (1992).

[18] Ya. Zel'dovich and S. S. Gershein, Sov. Phys. Usp. **3**, 593 (1961) [Usp. Fiz. Nauk **71**, 581 (1960)].

[19] S. Hara and T. Ishihara, Phys. Rev. A **40**, 4232 (1989).

[20] J. E. Pollard, D. J. Trevor, J. E. Reult, Y. T. Lee, and D. A. Shirley, J. Chem. Phys. **77** (1), 34 (1982).